# Dynamic light-scattering study of the glass transition in a colloidal suspension

W. van Megen
*Department of Applied Physics, Royal Melbourne Institute of Technology, Melbourne, Victoria 3000, Australia*

P. N. Pusey
*Royal Signals and Radar Establishment, St. Andrews Road, Malvern, WR14 3PS, England*
(Received 13 September 1990)

This paper describes a light-scattering study of the glass transition in nonaqueous suspensions of sterically stabilized colloidal spheres. The observed phase behavior, fluid, crystal, and glass, is consistent with an essentially hard-sphere interaction between the particles. Metastable fluid states were obtained upon shear melting the crystalline phases by tumbling the samples. Their intermediate scattering functions, measured by dynamic light scattering, showed the emergence of a nondecaying component, implying structural arrest, at essentially the same concentration as that at which homogeneously nucleated crystallization was no longer observed. The overall forms of the intermediate scattering functions are consistent with the predictions of mode-coupling theories for the glass transition. Supplementary studies of the static structure factors indicated only short-ranged spatial order for particle concentrations ranging from the equilibrium fluid through the metastable fluid to the glass.

## I. INTRODUCTION

In this paper, we describe studies by dynamic light scattering of the glass transition in suspensions of nearly equal sized hard colloidal spheres. This is arguably the simplest system to show a glass transition. We exploit the large characteristic relaxation times of colloidal systems to perform experiments on metastable states that are not possible (except for computer simulations) with atomic fluids.

The glass transition (GT) is a subject of long-standing interest;[1,2] its study has recently gained impetus with the application of mode-coupling theories,[3–7] developed initially to describe the dynamics of critical and equilibrium fluids. These theories are applied to metastable fluids at densities greater than their freezing point and crystallization is assumed not to occur. Calculation of the dynamics of the system then leads to the prediction of a well-defined density at which freezing into an amorphous solid phase occurs, i.e., a glass transition is found. Detailed predictions for the dynamical behavior of density fluctuations in both the metastable fluid and glassy states are obtained. To date, these theories have been applied mainly to simple one-component systems, such as hard-sphere[4,7] or Lennard-Jones[5] atoms. However, essentially all naturally occurring glasses are composed either of mixtures or of aspherical molecules whose crystallization has been avoided on cooling by the hindering of rotational motion or the formation of randomly bonded networks. One-component (atomic) systems cannot, in practice, be cooled rapidly enough to bypass crystallization and still be held controllably in metastable states. This limitation does not apply to colloidal systems for which long-lived metastable states can be reliably prepared.

The static[8,9] and dynamic[9–11] properties of assemblies of colloidal spheres suspended in a liquid have many features in common with atomic fluids. In particular, with increasing particle concentration, fluid, crystalline, and glassy phases are observed.[12,13] On time scales that are short compared with the time between collisions, the dynamics of atoms and colloidal particles are fundamentally different; atoms undergo free flight whereas colloidal particles execute (hydrodynamically hindered) diffusion.[10,11] However, on time scales over which many collisions occur, the motions in each case can be regarded as "interactive diffusion."[14] Colloidal particles are typically $10^3$ times larger than atoms. Thus, while the characteristic long-time relaxation rate of density fluctuations in an atomic fluid is of order $10^{11}$ s$^{-1}$, that of fluctuations in a colloidal suspension is of order 1 s$^{-1}$. The experiments discussed here exploit two important consequences of this essentially macroscopic relaxation time of a colloidal system. First, it is easy to drive the system into a metastable state by, for example, a mixing process which provides shear rates that exceed the system's rate of relaxation.[15] Second, once the metastable state is achieved it persists for many relaxation times before significant crystallization occurs.

Previous studies[12,13,16–19] have established that particles of the type used in this work have essentially hard-sphere interactions. This paper is mainly concerned with the application of dynamic light scattering (DLS) which provides the intermediate scattering function $f(Q,\tau)$ [Eqs. (2.6) and (2.7)], the time correlation function of the $Q$th spatial Fourier component of fluctuations in the particle number density. Our measurements span a range of concentration which includes the equilibrium fluid, metastable fluid, and glassy states. Qualitatively, our results

are in agreement with predictions of mode-coupling theory and computer simulation. Furthermore, for some properties we find essentially quantitative agreement with the mode-coupling calculations of Bengtzelius, Götze, and Sjölander;[4,5] the following paper[20] in this issue gives a more comprehensive comparison of our data with mode-coupling theory.

The idea that an assembly of spheres should show a GT dates back at least to the macroscopic sphere packing experiments of Bernal[21] and Scott[22] and the free volume model of Cohen and Turnbull.[23] Subsequent computer simulations[2,24,25] and the recent mode-coupling theories have led to a picture of the fundamental processes in terms of "neighbor cages" to which the motions of individual particles are partially or completely constrained. In the equilibrium fluid a particle is able to diffuse over long distances although its motion is continually hindered by temporary entrapments in cages formed by its current nearest neighbors. As the density of the fluid is increased towards the GT, the escape of a particle from its current cage requires the increasingly cooperative motion of its neighbors. The probability of such an escape approaches zero at the GT. Then, although they retain some freedom for local motions (within their cages), the particles are essentially localized or trapped. Furthermore, the onset of this localization occurs over a relatively narrow range of particle concentrations. Associated with the concomitant huge reduction of the long-time self-diffusion coefficient (and the divergence of the shear viscosity of the system) is the partial "freezing in" of density fluctuations on all spatial scales. Thus the amorphous solid or glass so formed can be viewed as a "structurally arrested" dense fluid.

At concentrations well below the GT the time taken for density fluctuations to relax fully (the "structural relaxation time") is small. Thus many complete fluctuations are observed in the course of a typical experiment and the time average, inherent in a measurement, is equivalent to its ensemble average, i.e., the system is ergodic. However, as the particle concentration is increased, the structural relaxation time increases and, at some stage, exceeds the duration of the experiment. In this case time and ensemble averages will differ and the system is effectively nonergodic.[1] From a practical point of view, in this nonergodic situation, the structural relaxation time can be regarded as infinite.

This paper, which presents a significantly more detailed account than two preliminary reports,[26,27] is set out as follows: In the next section we discuss sample preparation and experimental procedures, including the application of DLS to nonergodic systems. The results are presented in Sec. III followed by a discussion of the results in Sec. IV, where we also make largely qualitative comparisons with mode-coupling theory and comment on another experiment that has measured the intermediate scattering function near the glass transition. While the emphasis is on particle dynamics near the GT, we also show, in Sec. III, some measurements by static light scattering of the static structure factors of the fluid, metastable fluid, and glassy states.

## II. EXPERIMENTAL DETAILS

### A. Sample preparation

The particle suspensions used here are similar to those described in several previous studies.[12,13,16–19] The particles consisted of poly-(methylmethacrylate) (PMMA) spheres coated with chemically grafted layers of poly-(12-hydroxystearic acid) (PHSA) to provide steric stabilization.[28] The particles were dispersed in a mixture of decalin and carbon disulfide, the composition of which was adjusted to render the suspensions nearly transparent but to still provide sufficient (single) scattering of light; the weight fraction of $CS_2$ in the mixture was 0.29 and its refractive index was about 1.51, which is close to that of the particles. Samples having accurately determined compositions by weight were prepared in optical cells (of dimension $1\times1\times3$ cm$^3$) by methods described elsewhere.[13,17,18] Measurements by DLS on dilute suspensions yielded an average hydrodynamic radius $R=170\pm5$ nm and a polydispersity,[29] defined as the standard deviation of the particle size distribution divided by the mean, of $0.045\pm0.01$. (Possible effects of this relatively small degree of polydispersity will be considered later where appropriate; in much of the discussion, the suspensions will, for simplicity, be regarded as effectively monodisperse.)

The main objective of this paper is a study of the metastable states of samples whose equilibrium states are crystalline. These metastable states were obtained by tumbling the samples extensively on a wheel rotating at a few Hz in the vertical plane. The efficacy of this procedure depends on two properties of the suspensions. First, because of their low number density (of order $10^{13}$ cm$^{-3}$), colloidal crystals are extremely weak mechanically.[30] Thus the stresses imposed by tumbling greatly exceed the yield stresses of the colloidal solids, which are therefore "shear melted."[15] Second, the rates of shear imposed are much greater than the rates of crystallization of the samples, by virtue of their large structural relaxation times (Sec. I). (The static structure factors shown in Fig. 1 are consistent with well-defined metastable fluid states that have only the short-ranged spatial correlations inevitable in a concentrated system.)

### B. Static light scattering

The measurements of the angular dependence of the average scattered intensity were made with a specially constructed, temperature-controlled, photometer comprising the following features: (i) Computer-controlled sweeping of angle; typically angular steps of $\frac{1}{4}°$ were used with a dwell time at each setting of one second; (ii) the optical arrangement included a laser beam and detector aperture which could be enlarged as necessary to render speckle noise effectively negligible; and (iii) as in the DLS experiments (see below) the light source was an intensity-controlled $Kr^+$ laser which could be operated in any one of the lines, 476.2, 530.9, 568.2, or 647.1 nm.

For $N$ identical rigid spheres the measured average

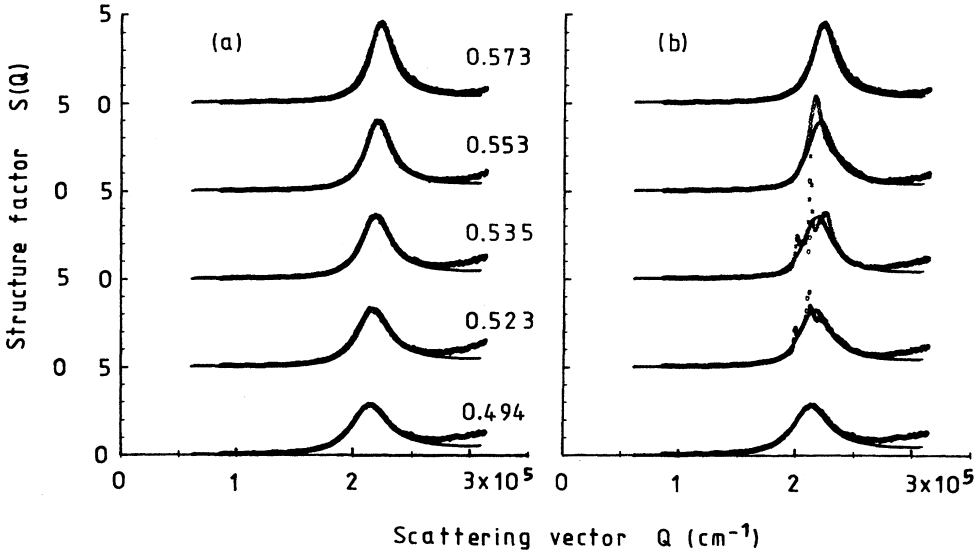


FIG. 1. Comparison of measured static structure factors $S(Q)$ (points), at effective hard-sphere volume fractions indicated, with predictions for hard spheres in the Percus-Yevick approximation (lines). (a) Measurements made immediately after randomization by tumbling the samples. (b) Measurements made several hours later. Bottom curve refers to the equilibrium fluid and top curve to the glass; samples at intermediate concentrations have crystallized. See text for further discussion.

scattered intensity $\langle I(Q)\rangle$ can be written as

$$\langle I(Q)\rangle = NP(Q)S(Q) , \tag{2.1}$$

where $P(Q)$ is the single-particle form factor and the static structure factor $S(Q)$ is

$$S(Q)=N^{-1}\sum_{j,k=1}^{N}\langle \exp[i\mathbf{Q}\cdot(\mathbf{r}_j-\mathbf{r}_k)]\rangle_E . \tag{2.2}$$

Here the scattering vector $\mathbf{Q}$ has magnitude

$$Q=(4\pi n/\lambda)\sin\theta/2 , \tag{2.3}$$

where $n$ is the refractive index of the medium, $\lambda$ is the wavelength *in vacuo*, $\theta$ is the scattering angle, $\mathbf{r}_j$ is the position of the $j$th particle, and $\langle\ \rangle_E$ indicates an ensemble average.

The form factor describes the average scattered intensity of a single particle. As mentioned above, the particles used in this study comprise a PMMA core and a thin PHSA shell which has a slightly different refractive index. Near index matching, i.e., when the difference between the average refractive indices of the particles and the suspension medium is small, the actual form of $P(Q)$ is a sensitive function of this difference, because of interference between the electric fields scattered by the core and the shell. In turn, the refractive-index difference depends strongly on both temperature and the wavelength of the illuminating radiation. It is therefore essential to measure $P(Q)$ for each sample individually at constant temperature and at all wavelengths used. In the present work this was achieved as follows; each sample was centrifuged at about 1000$g$ for several hours until the suspension separated into a compact sediment and a clear supernatant. By slowly rotating the samples on a vertical wheel for a short period, a small fraction of the particles was dispersed from the sediment into the supernatant. Measurement of the angular dependence of the intensity scattered from this dilute supernatant suspension provided estimates of the form factor $P(Q)$. Further extensive tumbling (for at least 12 h) then redispersed the particles completely so that measurements of $\langle I(Q)\rangle$ could be made for concentrated suspensions. Finally, estimates of the structure factors for the samples were obtained by using the measured $\langle I(Q)\rangle$ and $P(Q)$ in Eq. (2.1). Since, in this procedure, we have not attempted to determine the actual concentrations of the dilute supernatant suspensions, the resulting structure factors are in arbitrary units.

It should be emphasized that the decoupling of the scattered intensity into the product of form and structure factors of the particles, Eq. (2.1), is strictly valid only for rigid spherical particles which are identical in terms of both size and refractive-index profile. For polydisperse particles, the amplitudes of the fields scattered by the particles depend on their radii as do the correlations between their positions; then rigorous decoupling of the intensity is no longer possible. Nevertheless, for a polydisperse suspension, one can still determine a "measured" structure factor $S^M(Q)$ from the ratio of the intensities scattered by concentrated and dilute suspensions (see, e.g., Ref. 9, 31, and 32). For a polydispersity of 0.05, cf. 0.045 for the particles used here, the difference between $S^M(Q)$ and $S(Q)$, the structure factor for a monodisperse system at the same concentration, is not very large: at the freezing concentration (see Sec. III A) the amplitude of the main peak in $S^M(Q)$ is about 5% smaller than that in $S(Q)$.[9] Thus, since our main interest here is in the qualitative forms of the structure factors, we neglect the effect of polydispersity and use Eq. (2.1) for the data analysis.

### C. Dynamic light scattering

The optical arrangement and other basic details pertaining to the DLS experiments have been discussed in previous papers.[16–18] From DLS measurements[33,34] it is possible to obtain the normalized ensemble-averaged time correlation function of the intensity $I(Q,t)$ of the scattered light, defined by

$$g_E^{(2)}(Q,\tau)=\langle I(Q,0)I(Q,\tau)\rangle_E/\langle I(Q)\rangle_E^2 , \quad (2.4)$$

where $\tau$ is the correlation delay time. For the nonergodic samples [i.e., those whose relaxation times exceed the duration of an experiment (Sec. I)] special measures, discussed below, must be employed to obtain this ensemble average. In the case which applies in this work, where the range of spatial correlation between the particles is much smaller than the linear dimension of the scattering volume $V$, Eq. (2.4) can be written as

$$g_E^{(2)}(Q,\tau)=1+[cf(Q,\tau)]^2 . \quad (2.5)$$

Here

$$f(Q,\tau)\equiv F(Q,\tau)/S(Q) , \quad (2.6)$$

where $F(Q,\tau)$ is the (ensemble-averaged) intermediate scattering function of $N$ identical particles,

$$F(Q,\tau)=N^{-1}\sum_{j,k=1}^{N}\langle\exp\{i\mathbf{Q}\cdot[\mathbf{r}_j(0)-\mathbf{r}_k(\tau)]\}\rangle_E , \quad (2.7)$$

and $\mathbf{r}_j(t)$ is the position of particle $j$ at time $t$; the static structure factor $S(Q)$ is given by

$$S(Q)\equiv F(Q,0) . \quad (2.8)$$

In Eq. (2.5) $c$ is an experimental constant determined largely by the ratio of detector aperture to coherence area; in the usual practice of DLS the detector area is adjusted to be roughly equal to one coherence area and $c\approx 0.8$.[34]

The photon correlator used in these measurements did not have the multiple-sample-time facility available with more modern instruments. Thus, in order to capture the wide dynamic range of the highly nonexponential correlation functions encountered in this work, it was necessary to make separate measurements using several different sample times. In a preliminary report[26] we presented "raw" data in the form $cf(Q,\tau)$. Here, to facilitate comparison with theory, the measured data are divided by the constant $c$ to provide direct estimates of $f(Q,\tau)$. Correlation functions measured with different sample times were linked together by the following procedure. (i) For the shortest sample time ($10^{-4}$ s) $c$ was determined by extrapolation of the data to $\tau=0$. (ii) For measurements made with longer sample times $c$ was chosen to provide a good match of the data sets in their regions of overlap. For the more dilute samples, for which the intensity fluctuations were rapid, essentially the same value of $c$ was adequate at all sample times (implying that good estimates of the ensemble averages were obtained). However, for the more concentrated samples, the required value of $c$ varied somewhat from measurement to measurement; this is a consequence of the statistical uncertainty inherent in measurements on samples near the glass transition where the number density fluctuations decay slowly or are partly arrested.

As mentioned above, the nonergodicity of the more concentrated samples requires careful consideration to be given to the operation of the light-scattering technique. We have discussed DLS by nonergodic media in detail elsewhere;[35] here we summarize the points relevant to this work. For simplicity consider first a dense amorphous arrangement of many *stationary* particles (e.g., a glass at zero temperature). When illuminated by coherent laser light, the scattered intensity constitutes a random speckle pattern which is heavily modulated in space but constant in time. Each speckle (or coherence area) accepted by the detector represents a single spatial Fourier component of the number density. Clearly, in this extreme nonergodic case time averaging, inherent in the usual operation[33] of DLS, is pointless since there are no temporal intensity fluctuations. However, an ensemble average can still be effected through the acquisition of data from many independent scattering volumes within the medium, each of which gives rise to speckles of different intensities. If now the particles are allowed some freedom for local motion (as, for example, in a glass at nonzero temperature), small intensity fluctuations are superimposed on the previously constant speckle pattern, i.e., the new speckle pattern is composed of both constant and fluctuating components. In this case a single experiment samples only a restricted region of phase space associated with the local particle motions. Thus, as for the extreme nonergodic case, measurements on many independent volumes are still needed to provide a full ensemble average, i.e., an average that also includes the constant components of the speckle pattern (resulting from the frozen-in number density fluctuations) whose magnitudes may vary markedly from speckle to speckle. Finally, in the case of a fluidlike system of particles, in which diffusion over long distances occurs, a speckle undergoes many complete fluctuations in the course of an experiment so that time and ensemble averages are equivalent. This, of course, is the usual ergodic case.

Here, when studying the nonergodic samples, rather than performing the measurements on a very large number of independent volumes we adopted a less tedious approach. An enlarged scattering volume was obtained by using an unfocused laser beam and an enlarged detection slit. With this arrangement the detector aperture accepted about ten coherence areas in the scattered light field, corresponding to ten independent spatial Fourier components of the particle number density fluctuations. (Thus $c^2\approx 0.1$, i.e., $c\approx 0.33$, which can be compared with the value $c\approx 0.8$ applicable to the smaller scattering volume used for the ergodic samples.) Measurements, of $10^3$ s duration, were made for $M=10$ spatially separated scattering volumes, achieved by moving the sample between measurements. The mean intensities and unnormalized intensity correlation functions for the $M$ measurements were then summed and divided by $M$. It can be shown that in the limit $M\rightarrow\infty$ this procedure gives the full ensemble averages. Thus reasonable estimates of the ensemble averages should be obtained from our actual

measurements which effectively sample the time evolution of about 100 different Fourier components (ten coherence areas by ten scattering volumes). From this ensemble-averaged intensity correlation function the intermediate scattering function $f(Q,\tau)$ can be obtained with use of Eqs. (2.4) and (2.5). Nevertheless, in evaluating the DLS results it must be remembered that, although the data for the nonergodic samples appear quite smooth, they are subject to significant uncertainties due to the limited number of Fourier components included in the average. Measurements on a different set of 100 Fourier components (obtained by illuminating a different set of scattering volumes) could result in a significantly different estimate of $f(Q,\tau)$. (Since performing the measurements reported here we have developed the theory underlying a method by which the ensemble-averaged intermediate scattering function may be obtained from a single measurement of the time-averaged intensity correlation function.[35])

In the case of the more dilute samples, fluctuations in the intensity of scattered light are sufficiently rapid that essentially the full decay of $f(Q,\tau)$ to zero [or $g_E^{(2)}(Q,\tau)$ to one] can be measured in a single experiment. However, as the particle concentration is increased towards the GT the longest intensity fluctuation times increase to the extent that they exceed the duration of a practical experiment (i.e., the system becomes effectively nonergodic). Clearly for this case it is no longer possible to measure directly the full decay of $f(Q,\tau)$. Nevertheless, the existence of very large decay times can be deduced from the following considerations. Because of the limited range of intensity fluctuations observed in a single experiment on a nonergodic sample (see above), their magnitude $\lim_{\tau\to 0}\langle I(Q,0)I(Q,\tau)\rangle_T/\langle I(Q)\rangle_T^2$ will be less than $1+c^2$ (the value applicable for an ergodic sample [Eqs. (2.4) and (2.5)]); here $\langle\ \rangle_T$ denotes the time average inherent in a single measurement. Furthermore, both this magnitude of the fluctuations and the functional form of the measured (time-averaged) intensity correlation function will generally differ when different scattering volumes are studied, because of the different constant components of the speckle. In fact we use the observation of this behavior as a criterion to define the transition to nonergodicity.

In these experiments the sample times used ranged from $10^{-4}$ to $10^{-1}$ s and the duration of a single measurement was usually $10^3$ s. (For our 88-channel correlator this corresponds to a range of delay time $10^{-4}\leq\tau\leq 8.8$ s). Most measurements were made at a scattering vector $Q=2.17\times10^5$ cm$^{-1}$, which is close to $Q_m$, the positions of the main peaks in the static structure factors (see Fig. 1). For a few samples measurements were also made at $Q=1.36\times10^5$ cm$^{-1}$ ($<Q_m$) and $Q=3.48\times10^5$ cm$^{-1}$ ($>Q_m$).

## III. RESULTS

### A. Phase behavior

Table I gives details of the samples used in these experiments. The samples were tumbled, as described in Sec. II A, to provide thoroughly dispersed suspensions in metastable states. They were then left undisturbed for several days and the following phase behavior was observed. The most dilute sample A remained in a fluidlike phase. In samples B, C, and D small, homogeneously nucleated crystals formed and settled in about one day leaving clearly defined boundaries between coexisting colloidal crystal and colloidal fluid phases. By contrast, similar crystals formed in samples E and F did not settle and continued to occupy the entire volumes. In sample E crystallization was rapid (about one hour) whereas in sample F complete crystallization took more than a day. The more concentrated samples showed no sign of homogeneously nucleated crystallization. However, after several days partial crystallization, nucleated heterogeneously at the meniscus and the cell walls, was observed in samples G and H. We designated as "colloidal glasses" those samples G–J in which homogeneously nucleated crystallization appeared to be suppressed. (Photographs of suspensions showing roughly similar behavior have been published in Refs. 12 and 36).

After several days had elapsed, allowing full separation of the phases, the portion of the total volume occupied by the crystal in samples B, C, and D was plotted as a function of the weight fraction of PMMA in the suspensions.

TABLE I. Sample designations, effective hard-sphere volume fractions $\phi_E$, phases, first cumulants $\Gamma$, and relaxation times $T_L$.

| Sample | Our designation | $\phi_E$ | Phase | $\Gamma$ (s$^{-1}$) | $T_L$ (s) |
|---|---|---|---|---|---|
| A | 11(2) | 0.480 | Fluid | 49 | 0.093 |
| C* | 1* | 0.494 | Coexisting fluid | 41 | 0.16 |
| B | 11(3) | 0.504 | Fluid and crystal | 45 | 0.21 |
| C | 1 | 0.520 | Fluid and crystal | 43 | 0.46 |
| D | 2 | 0.529 | Fluid and crystal | 32 | 0.74 |
| E | 7 | 0.542 | Crystal | 34 | 9 |
| F | 3 | 0.554 | Crystal | 34 | $>10^3$ |
| G | 8 | 0.565 | Glass | 18 | $>10^3$ |
| H | 4 | 0.582 | Glass | 24 | $>10^3$ |
| I | 5 | 0.594 | Glass | | |
| J | 6 | 0.614 | Glass | 34 | |

Extrapolating the resulting straight line to 0% crystal and 100% crystal yielded a freezing concentration of 0.447 g/g and a melting concentration of 0.485 g/g. In order to provide a simple framework in which to discuss our data, we will, as in previous work,[12,13,17,18] adopt an effective hard-sphere model. Thus we assume that the effective volume fraction of the sample at freezing is $\phi_E=0.494$, the accepted value for hard-sphere fluids.[37] The effective volume fractions of the samples (listed in Table I) were then calculated by multiplying their measured weight fractions by 0.495/0.447. We note, however, that this procedure gives an effective hard-sphere melting volume fraction of 0.536 which is lower than the known value (0.545) for hard-sphere crystals.[37] This difference is probably caused by complications associated with slow gravitational settling of the particles. In a more recent study of suspensions of similar PMMA particles Paulin and Ackerson[19] devised a method to allow for gravitational settling and found good agreement between measured and theoretical values of the volume fraction at melting.

### B. Static structure factors

Our initial study[26] of the glass transition involved the determination of the phase behavior and the DLS measurements discussed below. Since then we have also determined the structure of the crystalline phases.[38] A by-product of the latter work was the measurement of the static structure factors of the metastable phases obtained immediately after extensive tumbling of the samples. In the nine months that elapsed between preparation of the samples and the structure factor measurements, a small, but known (by weighing), amount of liquid evaporated despite tight sealing of the sample cells. Thus it was necessary to recalculate the effective hard-sphere volume fractions of these samples (see Fig. 1).

Figure 1(a) shows the structure factors of the metastable fluids obtained by the procedures discussed in Sec. II B. For reasons mentioned there, the results for $S(Q)$ are in arbitrary units which differ from sample to sample. In order to present the data in a consistent form they have been scaled as follows. Structure factors were calculated from the Percus-Yevick (PY) theory for hard spheres; to allow partially for the known overestimation of the structure by simple PY theory the volume fractions $\phi'$ used in these calculations were given by

$$\phi'=\phi_E-\phi_E^2/16 , \tag{3.1}$$

the empirical correction suggested by Verlet and Weis.[39] The data were then scaled so that the amplitudes $S(Q_m)$ of their primary maxima coincided with the PY prediction. The abscissas were also scaled by a single factor to give coincidence of the experimental and PY peak positions. As can be seen in Fig. 1(a), there is reasonably good agreement between experiment and "theory" except for $Q>Q_m$ where the particle form factors $P(Q)$ have deep minima and measurements of $S(Q)$ become unreliable (see, for example, Ref. 9).

For completeness we show, in Fig. 1(b), the structure factors measured on the same samples after an equilibration period of several hours following slow tumbling. The equilibrium fluid at $\phi_E=0.494$, of course, shows no change. In this time the samples at $\phi_E=0.523$ and 0.535 have crystallized. The powder patterns for each of these samples show a sharp Bragg reflection and a broader but structured band of diffuse scattering. As discussed in detail elsewhere,[38] these features imply a random-stacked, close-packed structure for hard-sphere colloidal crystals. The structure factor of the sample at $\phi_E=0.553$ is consistent with a polycrystal containing very small crystallites so that strong diffraction broadening of the Bragg reflection is observed. At the highest concentration studied, $\phi_E=0.573$, the structure factor shows no change with time, implying that the sample is trapped in an amorphous or glassy state.

### C. Dynamic light-scattering results

All DLS measurements for the samples B–H were made after extensive tumbling which ensured thorough mixing and shear melting of any crystals. Hence they apply to the metastable fluid phases which exist prior to any significant crystallization. (Samples D and E, which crystallized quite rapidly, were retumbled between measurements.) In addition, the equilibrium fluid, sample A ($\phi_E=0.480$), and the coexisting equilibrium fluid, sample C* ($\phi_E=0.494$), were studied. For the latter sample C was used after it had stood long enough, about one day, for phase separation to occur.

Figure 2 shows plots of $\ln f(Q_m,\tau)$ against delay time $\tau$, where $f(Q_m,\tau)$ is the normalized intermediate scattering function defined by Eqs. (2.6) and (2.7), for all measurements made near the peaks $Q\approx Q_m$ of the static structure factors. The curves are labeled by sample designation and (effective hard-sphere) volume fraction. Four figures [2(a)–2(d)] cover different ranges of delay time and different fractions of the total decay. Figure 3 shows similar plots for samples E and G which include data measured not only at $Q\approx Q_m$ but also at scattering vectors above and below the peak in $S(Q)$.

It can be seen that the analysis procedure described in Sec. II C generally provides good overlap of data measured with different sample times. However, for a few cases, in particular sample G in Fig. 2(a) and sample F in Fig. 2(c), some mismatch is evident. This is a consequence of the limited statistical accuracy inherent in averaging over only about 100 Fourier components in these nonergodic samples (see Sec. II C).

Table I lists the initial decay rates or first cumulants $\Gamma$, defined by

$$\Gamma=-\lim_{\tau\to 0}\frac{d}{d\tau}\ln f(Q,\tau) , \tag{3.2}$$

of the intermediate scattering functions measured at $Q\approx Q_m$. These were obtained by standard analyses[40] of correlation functions measured with the (shortest) sample time, $10^{-4}$ s. For the reasons mentioned above, the statistical accuracy of these cumulants is poorer at the higher concentrations.

For samples A–E the time constants $T_L$ of the long-

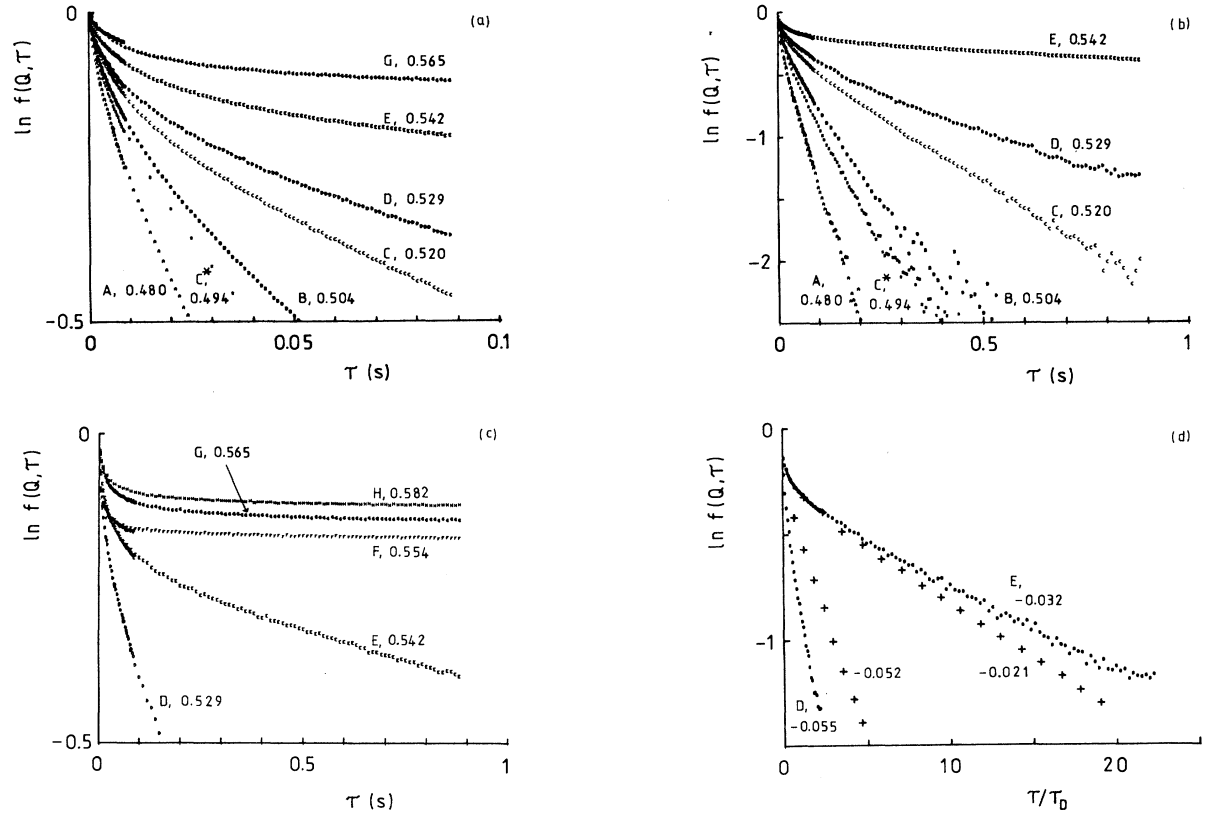


FIG. 2. Logarithms of the normalized intermediate scattering functions $f(Q_m,\tau)$, measured near the main peaks, $Q \approx Q_m$, in the static structure factors, vs delay time $\tau$. In (a)–(c) curves are labeled by sample designation and effective hard-sphere volume fractions $\phi_E$. (a) and (b) show data for the equilibrium and metastable fluids for different ranges of delay time; (a) also includes data for the glassy sample G. (c) shows the more concentrated metastable fluid and glassy phases. In (d) data for the two most concentrated metastable fluid samples D and E (points) are compared with calculations for Lennard-Jones atoms [crosses, taken from curves *d* and *e* of Fig. 2 of Bengtzelius (Ref. 5)]; here $\tau_D$ is the structural relaxation time, Eq. (4.1), and the curves are labeled by the separation parameter, Eq. (4.7). The experimental results are the same as those shown in (b) for samples D and E, except that for E data are shown for which $\tau$ extends to 8.8 s.

time decays of $f(Q,\tau)$ were estimated from their slopes in Fig. 2. As is evident from Table I these time constants are much smaller than the duration of one measurement ($10^3$ s); thus samples A–E may be designated as ergodic. For samples F–J DLS measurements on different scattering volumes gave differing results. As discussed in Sec. II C this observation indicates the presence of components in $f(Q,\tau)$ which decay on time scales longer than the duration of one measurement, i.e., $T_L > 10^3$ s. Therefore these samples are effectively nonergodic and, to obtain $f(Q,\tau)$, it was necessary to use the special measurement procedures outlined in Sec. II C.

## IV. DISCUSSION

### A. General aspects

First the static structure factors, shown in Fig. 1, for the metastable fluid states are discussed briefly. We reiterate that Fig. 1(a) does not constitute a rigorous comparison between experiment and theory. As mentioned in Sec. II B, the measured structure factors are in arbitrary units and, in addition, the theoretical curves take no account of the spread in particle size. Nevertheless, the significant feature of the results displayed in Fig. 1(a) is that in the range of particle concentration from the equilibrium fluid to the glass there is no structural change aside from slight narrowing and shifting of the peaks consistent with the compression of an amorphous arrangement of spheres. This finding supports the view that the GT is largely dynamic rather than structural in nature.[6]

As can be seen in Figs. 2 and 3, the intermediate scattering functions, $f(Q,\tau)$, all show initial rapid decays followed by significantly slower, roughly exponential, decays at long times. The decay rates $\Gamma_L$ ($\equiv T_L^{-1}$, see Table I) of the slower components depend strongly on the particle concentration and tend to zero (corresponding to decay times $T_L > 10^3$ s) at $\phi_E \approx 0.55$. On the other hand, the rates of initial decay $\Gamma$, or first cumulants (Table I), show a much weaker variation up to the highest concentration, $\phi_E = 0.614$, studied. These experimental findings are in qualitative agreement with studies of metastable

fluids composed of Lennard-Jones atoms by both computer simulation[25] and mode-coupling theory.[5,6]

The rapid initial decays of $f(Q,\tau)$ can be associated with the local motions of particles (or atoms) within their nearest-neighbor cages (see Sec. I). The slower decays at longer times reflect the more hindered diffusion of the particles over longer distances. With increasing concentration such large excursions become increasingly unlikely. At the GT the particles become effectively trapped by their neighbors ($T_L \rightarrow \infty$) and number density fluctuations of all wavelengths become partly frozen in. Nevertheless, the weak concentration dependence of the initial decay rates $\Gamma$ indicates that, even above the GT, the particles still have significant freedom for local motion.

An important feature of these experiments is the correlation between the macroscopically observed phase behavior and the microscopic dynamics revealed by DLS. We find that, while the ergodic sample E ($\phi_E = 0.542$) crystallized completely within an hour or two after tumbling, sample F ($\phi_E = 0.554$), the first to show decay times in excess of $10^3$ s, took a day or more for complete crystallization. The next sample G ($\phi_E = 0.565$) did not show homogeneously nucleated crystallization over several weeks. We therefore identify $\phi_G = 0.560 \pm 0.005$ as the volume fraction at which the GT occurs in our suspensions.

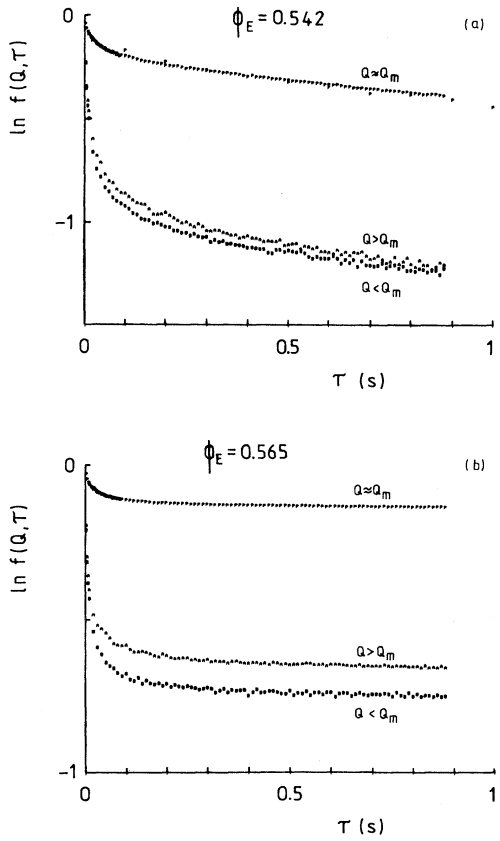


FIG. 3. Logarithms of the normalized intermediate scattering functions vs delay time at different scattering vectors: Top curves $Q = Q_m$; middle curves, $Q = 1.60 Q_m$; bottom curves, $Q = 0.63 Q_m$. (a) Metastable fluid sample E, $\phi_E = 0.542$; (b) glassy sample G, $\phi_E = 0.565$.

This value of $\phi_G$ is somewhat lower than that, 0.58–0.60, found in both computer simulation of hard spheres[24] and an earlier study of a similar colloidal system.[12] The reasons for this discrepancy remain to be established. It has been suggested[41] that a sufficiently broad distribution of particle size can cause suppression of crystallization in a manner which could be confused with a genuine glass transition in a monodisperse system. However, following a suggestion by Ackerson,[42] we subjected the glassy samples G–I (which did not show homogeneously nucleated crystallization when left undisturbed) to a small oscillatory shear, achieved by rocking the sample cells. The stress imposed by this procedure caused the top parts of the samples to flow while the bottom parts remained stationary relative to the cells. In the narrow region separating the flowing and stationary portions, formation of crystallites was observed after a few cycles of oscillation. Presumably the shear flow in this region was adequate to aid the local rearrangement of the particles required for crystallization. This observation indicates that it is indeed structural arrest, associated with the GT, rather than polydispersity which suppresses crystallization in the undisturbed samples. Nevertheless, polydispersity may affect the actual value of $\phi_G$.

### B. Comparison with mode-coupling results

There are relatively few results in the literature with which our data can be compared quantitatively. However, numerical evaluations of mode-coupling theory of the intermediate scattering function $f(Q,\tau)$ have been reported for both hard spheres[4,7] and Lennard-Jones atoms.[5] Here we discuss briefly aspects of our results in light of this work; a more comprehensive analysis is given in the following paper.[20]

A quantity for which a direct comparison between experiment and theory can be made is $f(Q,\infty)$, the amplitude of the frozen-in component of the number density fluctuations in the glass phase. Since this is effectively a structural property one might expect the theory developed for hard-sphere atoms to apply to hard-sphere colloids. Figure 3(b) shows intermediate scattering functions $f(Q,\tau)$ for sample G, the lowest-concentration glass, for scattering vectors $Q$ below, at, and above the primary maximum in the static structure factor $S(Q)$. In each case, after an initial rapid decay, $f(Q,\tau)$ becomes essentially independent of time, as expected for a glass. We estimate $f(Q,\infty)$ from the plateau levels of these curves. This quantity, plotted as a function of $Q$ in Fig. 4, is in good agreement with the theoretical prediction of Bengtzelius, Götze, and Sjölander[4] for hard spheres at the GT concentration. Nevertheless, because there is probably further residual relaxation of $f(Q,\tau)$ for $\tau > 1$ s, these experimental values of $f(Q,\text{“}\infty\text{”})$ may be slightly overestimated.

A direct comparison between the dynamic properties of colloidal particles in suspension and those of atomic systems is not straightforward for the following reasons.

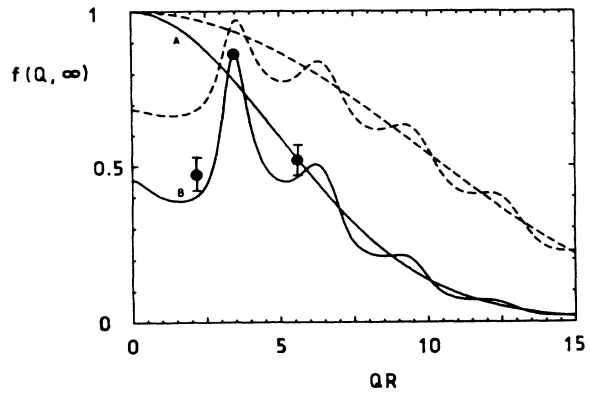


FIG. 4. Dependence on the scattering vector $Q$ ($R$ is the particle radius) of the amplitude $f(Q,\infty)$ of number density fluctuations which are frozen in at the glass transition. Data points are taken from the "plateau" values in Fig. 3(b), which refers to the glassy sample G at $\phi_E=0.565$; solid curve $B$ is the mode-coupling prediction (Ref. 4) for hard spheres at $\phi=\phi_G$. (Solid curve $A$ is the mode-coupling prediction for the frozen-in component of the self-intermediate scattering function of hard spheres at $\phi=\phi_G$. The dashed lines are theoretical predictions for the frozen-in components of the coherent and self-intermediate scattering functions of a higher-concentration glass, separation parameter [Eq. (4.7)], $\sigma=0.066$. See Ref. 4 for further details.)

The dynamics of particles in suspension are diffusive on all relevant time scales. However, as discussed in Sec. IV A, there is a demarcation between short-time local and long-time large-scale motions. On the other hand, the dynamics of atoms are ballistic at short times, but their long-time motions are also diffusive (see Sec. I). Since it is this large-scale diffusive motion which ceases at the GT, it seems plausible that there is an underlying similarity between the two cases. Such an analogy between the long-time diffusive dynamics of atomic fluids and colloidal suspensions has recently been discussed by de Schepper *et al.*[14] On this basis we attempt a quantitative comparison by defining a characteristic relaxation time $\tau_D$ as

$$\tau_D=R^2/6D_T \ , \tag{4.1}$$

where $R$ is the radius of the particle (or atom) and $D_T$ is its long-time self-diffusion coefficient (i.e., $\tau_D$ is the time taken by a particle to diffuse a distance equal to its radius). The highest concentration at which reliable values of $D_T$, for both hard-sphere colloids and hard-sphere atoms, are available is at freezing ($\phi_E=0.494$); we therefore use these values to determine $\tau_D$. Other experiments[18] on similar colloidal systems have shown that, at freezing, $D_T\approx 0.013D_0$, where $D_0$ is the low-concentration (Stokes-Einstein) diffusion constant. For the particles used in this study $D_0=9.35\times10^{-9}$ cm$^2$ s$^{-1}$, giving $D_T=1.22\times10^{-10}$ cm$^2$ s$^{-1}$ which, with $R=170$ nm, gives

$$\tau_D=0.4 \text{ s} \ . \tag{4.2}$$

Computer simulations[24] of hard-sphere atomic fluids give, at freezing,

$$D_T=2.13\times10^{-2}(\delta^2 k_B T/m)^{1/2} \ , \tag{4.3}$$

where $\delta$ ($=2R$) is the diameter of the atom, $m$ its mass, and $k_B T$ is the thermal energy.

The only work which includes extensive computations of $f(Q,\tau)$ for an atomic system is that of Bengtzelius,[5] who studied Lennard-Jones atoms. He presented his results in terms of a scaled time $\tau/\tau_0$, where

$$\tau_0=(m\delta^2/\varepsilon)^{1/2} \tag{4.4}$$

and $\varepsilon$ is the Lennard-Jones energy parameter. Since we do not know $D_T$ at freezing for this system, we estimate $\tau_D$ from Eq. (4.1) by eliminating $m$ from Eqs. (4.3) and (4.4) so that

$$\tau_D=1.96(\varepsilon/k_B T)^{1/2}\tau_0 \ . \tag{4.5}$$

Taking $k_B T/\varepsilon=0.6$ and $\tau_0=2.15\times10^{-12}$ s, the values used in the calculations, gives

$$\tau_D=2.52\tau_0=5.42\times10^{-12} \text{ s} \ . \tag{4.6}$$

Following Bengtzelius we also define, as a measure of the "distance" of a sample (colloidal or atomic) from the GT, the "separation parameter"

$$\sigma=(\phi_E-\phi_G)/\phi_G \ . \tag{4.7}$$

Figure 2(d) shows intermediate scattering functions in terms of the scaled time $\tau/\tau_D$ [Eq. (4.2)] for samples D ($\sigma=-0.055\pm0.01$) and E ($\sigma=-0.032\pm0.01$). These are the samples closest to the GT which still show a reasonable fraction of the full decay of $f(Q,\tau)$. Also shown in Fig. 2(d) are the results of Bengtzelius, taken from Fig. 2 of Ref. 5, for $\sigma=-0.052$ and $-0.021$; in this case the scaled time was calculated from Eq. (4.6). It can be seen that both experimental and theoretical intermediate scattering functions have similar forms. The dependence of $f(Q,\tau)$ on concentration is somewhat weaker for the atomic system. This may be associated with the softness of the atomic pair potential[43] and/or the effects of hydrodynamic interactions in the colloidal suspensions. Nevertheless, in view of the uncertainties involved in this comparison, it is striking that such disparate systems show such similar behaviors.

We now consider the functional form of the intermediate scattering functions $f(Q,\tau)$ in more detail. In the literature on molecular glasses the long-time (low-frequency) relaxation associated with the final breakdown of cages and the onset of long-distance diffusion is usually called the "$\alpha$ relaxation." In many cases this process, which can be studied by other techniques such as dielectric relaxation and neutron scattering, is found to show a "stretched-exponential" decay, $\exp[-(t/\tau_c)^\beta]$;[1,44,45] here $\tau_c$ is a characteristic time and $\beta$ is a parameter less than one. Mode-coupling theories[5,6] predict that for concentrations well below $\phi_G$ the long-time relaxation of $f(Q,\tau)$ is close to single exponential, $\beta\approx1$, whereas for $\phi_E$ close to $\phi_G$ significant stretching is found with $\beta$ taking a value as small as 0.5. Inspection of Fig. 2 shows that the experimental intermediate scattering functions

show roughly exponential long-time decays (straight lines in this log-linear representation), as do the theoretical functions[5] shown as crosses in Fig. 2(d). In view of the inevitable statistical uncertainties, discussed in Sec. II C, we do not wish to suggest more than that these long-time data fit a stretched exponential with $\beta=0.9\pm0.1$ (see Fig. 6 of Ref. 20 for a more detailed analysis of these data in terms of the $\alpha$ relaxation). Finally we note that much closer to the GT Bengtzelius[5] found $\beta=0.88$ for Lennard-Jones atoms at $Q=Q_m$.

Some studies[5,6] of atomic systems also reveal the emergence, close to the GT, of a secondary relaxation process, the "$\beta$ relaxation," which takes place on a time (or frequency) scale intermediate between those of the short-time local motions and the long-time $\alpha$ relaxation. This $\beta$ relaxation can be viewed as reflecting a relatively slow structural rearrangement of the particle cages. In the mode-coupling theory it is usual to plot the intermediate scattering functions in the form $f(Q,\tau)$ versus the logarithm of time (see Fig. 5). Here the signature of the $\beta$ relaxation is a change in the sign of the second derivative, $d^2f/(d\ln\tau)^2$, prior to the onset of $\alpha$ relaxation. Referring to Fig. 5(a) we see that for $\phi_E<0.529$ $-\mathrm{df}/d\ln\tau$ increases continuously with $\ln\tau$. However, for $\phi_E=0.542$ there is a region of at least one decade in time where the slope is almost constant, i.e., $d^2f/(d\ln\tau)^2=0$, which may suggest the onset of an observable $\beta$ relaxation. Indeed in measurements made below the peak in the static structure factor [Fig. 5(b)] the relaxation curve for this sample ($\phi_E=0.542$) shows a distinct decrease in the slope $-df/d\ln\tau$ after its initial increase. (See the following paper[20] for a more detailed analysis of these data in relation to mode-coupling theory and the $\beta$ relaxation.)

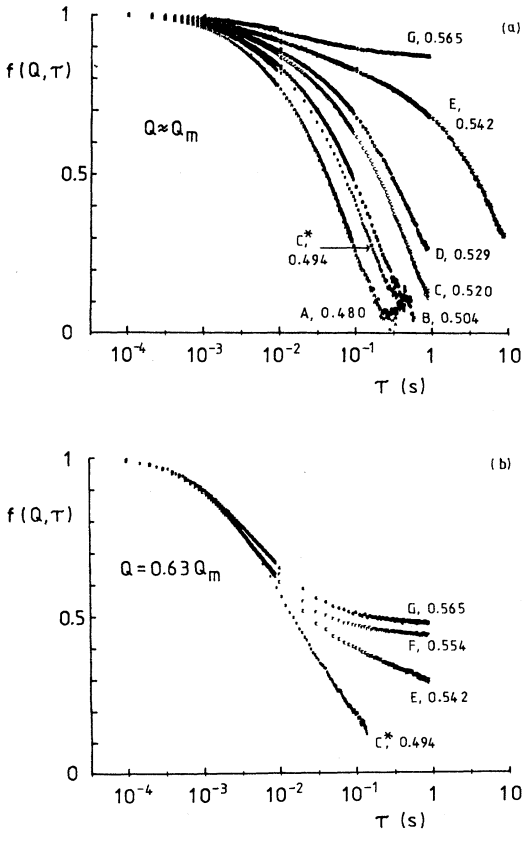


FIG. 5. Normalized intermediate scattering functions vs logarithm of time. (a) Measurements made at $Q=Q_m$ (these are the same data as shown in Fig. 2 except that the measurement for sample E was extended to delay time $\tau=8.8$ s); (b) measurements made at $Q=0.63Q_m$.

We note that, while the $\alpha$ relaxation is not observed in the glass state (since long-distance diffusion is suppressed), the $\beta$ relaxation persists and is responsible for the slow approach of $f(Q,\tau)$, seen in Fig. 5, to its long-time asymptote $f(Q,\infty)$ for $\phi_E=0.565$.

### C. Comparison with a DLS study of a microemulsion

Chen and co-workers[46,47] reported a DLS study of water-in-oil microemulsion droplets of radius $R=5$ nm over a wide range of concentration. Because of the small radius their measurements apply to the low-$Q$ regime, $QR\approx0.1$, whereas our experiments and most of the detailed theory and computer simulation work were performed at scattering vectors near the main peak in the structure factor, $QR\approx3.5$. Their correlation data could be fitted well by stretched exponentials. Both the parameter $\beta$ and the first cumulant (or initial slope) $\Gamma$ of the correlation functions showed minima at a volume fraction of about 0.65 which was identified as the glass transition concentration $\phi_G$. We make the following remarks about this work.

(i) The polydispersity of the droplets was stated to be about 0.25 (which can be compared with 0.045 for our particles). Thus crystallization was suppressed[41] so that direct comparison with observed phase behavior was not possible.

(ii) At the small values of $QR$ applying in this work this degree of polydispersity gives rise to a strong incoherent component in the measured correlation functions. For a polydispersity of 0.25 and volume fraction of 0.5, the theory of Ref. 32 predicts a relative incoherent amplitude of about 0.6. The presence of both coherent and incoherent contributions will have a considerable effect on the concentration dependence of $\Gamma$ and the nonexponentiality of the measured correlation functions. It is worth noting that, in an earlier study of a microemulsion system,[48] a concentration dependence of $\Gamma$ similar to that found by Chen and co-workers up to $\phi_E=0.6$ was explained entirely in terms of polydispersity (and a hard-sphere model). In the simplest form of this theory $f(Q,\tau)$ is predicted to be the sum of two exponentials, the coherent component, which describes collective motions, and the incoherent component describing single-particle motions;[32] while the decay rate of the former is only weakly dependent on concentration, that of the latter decreases rapidly with increasing concentration due to increasingly effective caging. We point out that such a function, with the inclusion of typical experimental noise, can be fitted approximately by a stretched exponential over a limited range of decay. In their second paper Chen and co-workers[47] argued that the observation of a

roughly single-exponential decay at low concentrations implied that polydispersity could not cause significant nonexponentiality at high concentrations. This claim overlooks the effect of incoherent scattering, described above, which was established several years ago both experimentally and theoretically.[32] (Note that in our experiments incoherent scattering was negligible, or at least small, for two reasons: the much smaller polydispersity and the dominant coherent scattering at $Q \approx Q_m$.)

(iii) Chen and co-workers do not appear to have appreciated fully the difficulties encountered in studying nonergodic samples by DLS. In particular special measures must be taken to obtain an ensemble average (see Sec. II B). As we have discussed in detail elsewhere,[35] the time-averaged intensity correlation function obtained in a single measurement on a nonergodic sample is related to the ensemble-averaged function by an equation significantly more complicated than Eq. (2.5).

## V. CONCLUDING REMARKS

This paper describes light-scattering studies of suspensions of hard-sphere colloidal particles over a range of concentrations which spans the glass transition. While static structure is considered briefly (Secs. III B and IV A), emphasis is on the dynamics of the metastable fluid and glassy states, described by intermediate scattering functions (or the correlation functions of the particle density fluctuations) $f(Q,\tau)$. Qualitatively, the behavior of $f(Q,\tau)$ is consistent with that found in several theoretical and simulation studies of glass-forming systems. In addition, we have been able to make quantitative comparisons with some predictions of mode-coupling calculations of Bengtzelius and co-workers. Our main findings follow.

(i) As in previous work, fluid, crystalline, and glassy states of the suspensions were observed directly. The GT occurred at an effective hard-sphere volume fraction of $\phi_G = 0.56 \pm 0.005$.

(ii) There is no marked structural change associated with the GT. With increasing sample concentration, the static structure factors exhibit only slight narrowing and shifting of the peaks, consistent with the compression of an amorphous arrangement of spheres.

(iii) The intermediate scattering functions show initial, fairly rapid, decays associated with local particle motions, and slower decays at longer times, associated with larger-scale excursions. While the rates of the initial decays depend only weakly on concentration, those of the slower decays are strongly concentration dependent. In particular, as the GT is approached the time constants of the slow decays diverge, signaling structural arrest, the partial freezing in of number density fluctuations.

(iv) The amplitudes $f(Q,\infty)$ of the components frozen in at the GT are in quantitative agreement with those predicted by mode-coupling calculations on hard spheres, for values of $Q$ smaller than, equal to, and larger than the position $Q_m$ of the primary peak in the static structure factor (see Fig. 4).

(v) In order to compare quantitatively the dynamic properties of suspensions and atomic fluids a time scaling, based on the long-time single-particle diffusion in each system, was proposed. With the use of this time scaling reasonable agreement was found between the intermediate scattering functions measured on suspensions and those calculated from mode-coupling theory for Lennard-Jones atoms.

(vi) In these systems of essentially identical spheres we find that the intermediate scattering functions at long times can be fitted by weakly stretched exponentials ($\beta \approx 0.9$). It is possible that the strongly stretched-exponential relaxations of $f(Q,\tau)$ found in other systems (such as polymers[49] and mixed ionic glasses[50]) may be a consequence of their complexity.

(vii) We have noted qualitative indications of a significant $\beta$ process occurring on a time scale intermediate between those associated with the microscopic motions and the large-scale $\alpha$ relaxation. A detailed analysis of our data in terms of mode-coupling predictions of the $\beta$ relaxation is presented in the following paper.[20]

In this paper, when discussing the functional forms of the intermediate scattering functions $f(Q,\tau)$, we have concentrated on the quite extensive measurements made at the main peaks, $Q \approx Q_m$, of the static structure factors. Mode-coupling theories also make specific predictions concerning the $Q$ dependence of the various relaxation processes. A preliminary analysis[20] of the limited data taken at other values of scattering vector shows reasonable agreement with theory for sample E, $\phi_E = 0.542$ [data shown in Fig. 3(a)]. However, the long-time relaxation of $f(Q,\tau)$ for sample C*, $\phi_E = 0.494$, at $Q = 0.63 Q_m$ (data not shown here) was found to be significantly slower than that predicted. It is possible that at this value of $Q$, where $S(Q)$ is quite small (see Fig. 1), there is an incoherent contribution to the scattering, arising from the particles' polydispersity. As discussed in Sec. IV C, this contribution can cause a slow decay of the measured intermediate scattering function. We are currently investigating this possibility as part of more complete study of the colloidal glass transition.

We conclude with some remarks about the glass transition concentration $\phi_G$. For molecular systems the properties of the metastable liquid and glassy states are usually studied as functions of temperature. However, it seems that the important parameter which controls the GT is the density, rather than the temperature, of the system. Changing temperature is mainly a convenient way to change the density at constant pressure. Thus one can associate a conventional glass transition temperature with the density (or particle concentration) $\phi_G$.

Traditionally the temperature $T_G$ of the glass transition of molecular systems is defined as that at which the shear viscosity of the supercooled liquid reaches about $10^{14}$ poise. On heating a molecular glass from below $T_G$ a calorimetric anomaly (a peak in the heat capacity) is typically found at about the same temperature. Unfortunately, it is difficult to apply these criteria to colloidal systems. First, because of the large structural relaxation times $\tau_D$, it is difficult to measure their zero-shear viscosities; colloidal suspensions exhibit strong shear thinning at shear rates comparable to $\tau_D^{-1}$. Reliable zero-shear

viscosities have been reported only at suspension concentrations up to not much more than the freezing concentration. Second, because of the small number densities, the (excess) heat capacities are immeasurably small. Thus here we have used the observed suppression of homogeneously nucleated crystallization as the macroscopic indication of the glass transition.

For atomic systems the characteristic critical behavior of the microscopic dynamics, which leads to nonergodicity, is predicted by mode-coupling theories to occur at a temperature $T_C > T_G$ (or concentration $\phi_C < \phi_G$).[6] It is interesting that, in the colloidal suspensions, we find the onset of nonergodicity and the suppression of crystallization occurring at almost the same concentrations, i.e., $\phi_C \approx \phi_G = 0.56$ (see Sec. IV A); for this reason we have not, in this paper, distinguished between $\phi_G$ and $\phi_C$.

## ACKNOWLEDGMENTS

We thank W. Götze and L. Sjögren for several valuable discussions concerning the work reported here (see the following paper), B. J. Ackerson for an important suggestion (see Ref. 42), and S. M. Underwood for preparing the PMMA particles.

[1]J. Jäckle, Rep. Prog. Phys. **49**, 171 (1986); Philos. Mag. B **56**, 113 (1987).
[2]C. A. Angell, J. H. R. Clarke, and L. V. Woodcock, Adv. Chem. Phys. **48**, 397 (1981).
[3]E. Leutheusser, Phys. Rev. A **29**, 2765 (1984).
[4]U. Bengtzelius, W. Götze, and A. Sjölander, J. Phys. C **17**, 5915 (1984).
[5]U. Bengtzelius, Phys. Rev. A **34**, 5059 (1986).
[6]W. Götze, in *Liquids, Freezing and the Glass Transition,* Les Houches Session 51, 1989, edited by D. Lesvesque, J. P. Hansen, and J. Zinn-Justin (North-Holland, Amsterdam, 1991).
[7]J. L. Barrat, W. Götze, and A. Latz, J. Phys. Condens. Matter **1**, 7163 (1989).
[8]W van Megen and I. Snook, Adv. Colloid Interface Sci. **21**, 119 (1984).
[9]P. N. Pusey, in *Liquids, Freezing and the Glass Transition,* Les Houches Session 51, 1989, edited by D. Lesvesque, J. P. Hansen, and J. Zinn-Justin (North-Holland, Amsterdam, 1991).
[10]P. N. Pusey and R. J. A. Tough, in *Dynamic Light Scattering,* edited by R. Pecora (Plenum, New York, 1985).
[11]W. Hess and R. Klein, Adv. Phys. **32**, 173 (1983).
[12]P. N. Pusey and W. van Megen, Nature (London) **320**, 340 (1986).
[13]P. N. Pusey and W. van Megen, in *Physics of Complex and Supramolecular Fluids,* edited by S. A. Safran and N. A. Clark (Wiley, New York, 1987).
[14]I. M. de Schepper, E. G. D. Cohen, P. N. Pusey, and H. N. W. Lekkerkerker, J. Phys. Condens. Matter **1**, 6503 (1989); P. N. Pusey, H. N. W. Lekkerkerker, E. G. D. Cohen, and I. M. de Schepper, Physica A **164**, 12 (1990).
[15]N. A. Clark and B. J. Ackerson, Phys. Rev. Lett. **44**, 1005 (1980).
[16]P. N. Pusey and W. van Megen, J. Phys. (Paris) **44**, 285 (1983).
[17]W. van Megen, R. H. Ottewill, S. M. Owens, and P. N. Pusey, J. Chem. Phys. **82**, 508 (1985).
[18]W. van Megen and S. M. Underwood, J. Chem. Phys. **91**, 552 (1989).
[19]S. E. Paulin and B. J. Ackerson, Phys. Rev. Lett. **64**, 2663 (1990).
[20]W. Götze and L. Sjögren, following paper, Phys. Rev. A **43**, 5442 (1991).
[21]J. D. Bernal, Nature (London) **183**, 141 (1959); **185**, 68 (1960); Proc. R. Soc. London, Ser. A **280**, 299 (1964); J. D. Bernal and J. Mason, Nature (London) **188**, 910 (1960).
[22]G. D. Scott, Nature (London) **188**, 908 (1960); **194**, 956 (1962); **201**, 382 (1964); J. Chem. Phys. **40**, 611 (1964).
[23]M. H. Cohen and D. Turnbull, J. Chem. Phys. **31**, 1164 (1959); **34**, 120 (1961); **52**, 3038 (1970); Nature (London) **203**, 964 (1964); D. Turnbull, J. Phys. (Paris) Colloq. **35**, C4-1 (1974); G. Grest and M. H. Cohen, Adv. Chem. Phys. **48**, 455 (1981).
[24]L. V. Woodcock, Ann. N.Y. Acad. Sci. **37**, 274 (1981).
[25]J. J. Ullo and S. Yip, Phys. Rev. Lett. **54**, 1509 (1985); Phys. Rev. A **39**, 5877 (1989).
[26]P. N. Pusey and W. van Megen, Phys. Rev. Lett. **59**, 2083 (1987).
[27]P. N. Pusey and W. van Megen, Ber. Bunsenges. Phys. Chem. **94**, 225 (1990).
[28]L. Antl, J. W. Goodwin, R. D. Hill, R. H. Ottewill, S. M. Owens, S. Papworth, and J. A. Waters, Colloids Surf. **17**, 67 (1986).
[29]P. N. Pusey and W. van Megen, J. Chem. Phys. **80**, 3513 (1984).
[30]P. M. Chaikin, J. M. de Meglio, W. Dozier, H. M. Lindsay, and D. A. Weitz, in *Physics of Complex and Supramolecular Fluids,* edited by S. A. Safran and N. A. Clark (Wiley, New York, 1987).
[31]P. van Beurten and A. Vrij, J. Chem. Phys. **74**, 2744 (1981).
[32]P. N. Pusey, H. M. Fijnaut, and A. Vrij, J. Chem. Phys. **77**, 4270 (1982).
[33]B. J. Berne and R. Pecora, *Dynamic Light Scattering* (Wiley, New York, 1976).
[34]*Photon Correlation and Light Beating Spectroscopy,* edited by H. Z. Cummins and E. R. Pike (Plenum, New York, 1974); *Photon Correlation Spectroscopy and Velocimetry,* edited by H. Z. Cummins and E. R. Pike (Plenum, New York, 1977).
[35]P. N. Pusey and W. van Megen, Physica A **157**, 705 (1989).
[36]W. van Megen, P. N. Pusey, and P. Bartlett, Phase Trans. **21**, 207 (1990).
[37]W. G. Hoover and F. H. Ree, J. Chem. Phys. **49**, 3609 (1968).
[38]P. N. Pusey, W. van Megen, P. Bartlett, B. J. Ackerson, J. G. Rarity, and S. M. Underwood, Phys. Rev. Lett. **63**, 2753 (1989).
[39]L. Verlet and J. J. Weis, Phys. Rev. A **5**, 939 (1972).
[40]D. E. Koppel, J. Chem. Phys. **57**, 4814 (1972); J. C. Brown, P. N. Pusey, and R. Dietz, *ibid.* **62**, 1136 (1975).
[41]E. Dickinson and R. Parker, J. Phys. (Paris) Lett. **46**, L-229 (1985); J. L. Barrat and J. P. Hansen J. Phys. (Paris) **47**, 1547 (1986); P. N. Pusey, *ibid.* **48**, 709 (1987).
[42]B. J. Ackerson (private communication).
[43]B. Bernu, J. P. Hansen, Y. Hiwatari, and G. Pastore, Phys. Rev. A **36**, 4891 (1987); G. Pastore, B. Bernu, J. P. Hansen, and Y. Hiwatari, Phys. Rev. A **38**, 454 (1988).
[44]K. L. Ngai, Comments Solid State Phys. **9**, 127 (1979).
[45]G. Williams and D. C. Watts, Trans. Faraday Soc. **66**, 80

(1970).
[46]S. H. Chen and J. S. Huang, Phys. Rev. Lett. **55**, 1888 (1985).
[47]E. Y. Sheu, S. H. Chen, J. S. Huang, and J. C. Sung, Phys. Rev. A **39**, 5867 (1989).
[48]D. J. Cebula, R. H. Ottewill, J. Ralston, and P. N. Pusey, J. Chem. Soc., Faraday Trans. 1 **77**, 2585 (1981).
[49]D. Richter, B. Frick, and B. Farago, Phys. Rev. Lett. **61**, 2465 (1988).
[50]F. Mezei, W. Knaak, and B. Farago, Phys. Rev. Lett. **58**, 571 (1987).